Received: March 20, 2017
Revised: June 15, 2017
Accepted: June 16,2017

Effect of Thermal Conductivity of Carbon Superficial Layers on the Kinetics of Laser-Induced Incandescence

Kateryna Zelenska*, Serge Zelensky, Alexandr Kopyshinsky

Faculty of Physics, Taras Shevchenko National University of Kyiv, Kyiv 03127, Ukraine

Abstract

The effect of thermal conductivity on pulsed thermal emission, known as laser-induced incandescence (LII), of thin superficial layers of carbon samples with rough and polished surfaces was studied. LII was excited by irradiation of the carbon surfaces with nanosecond pulses of a YAG:Nd laser (1064 nm) with intensity of 3-40 MW/cm^2. The results of the oscilloscope measurements of the LII pulse shape and calculation data demonstrated a significant reduction in the duration (FWHM) of the thermal emission pulse and its prolonged decay. The observed phenomenon was attributed to an increase in the thermal conductivity of the superficial layers of carbon samples.

Keywords: Thermal emission, Laser-induced incandescence, Nanosecond laser pulses, Thermal emission relaxation, Thermal conductivity, Porous carbon, Polished carbon surface.

1. Introduction

Laser-induced incandescence (LII) is pulsed thermal emission of nanosecond duration, which is observed when light-absorbing materials are heated to peculiar incandescent temperatures under irradiation with high power nanosecond laser pulses. For carbon, it is several thousands of Kelvin that corresponds to its intensive sublimation. LII of soot microparticles in flames and engine exhaust gases [1-6], aqueous suspensions of carbon microparticles (carbon black suspensions, CBS) [7-10], polymers [11-12] and borate glass [13-14] doped by carbon microinclusions, carbon [15-16] and silicon [17] surfaces has been investigated and reported in numerous papers that indicates the relevance and importance of this study.

In previous research, LII was excited by a sequence of laser pulses and dependence of the LII intensity (LII signal integrated over time and over the irradiated sample surface) on the laser irradiation dose was studied. Evaporation of material of carbon microparticles in CBS led to a decrease in the LII intensity with an increase in the irradiation dose [10]. The LII intensity of carbon suspensions in polymers (polystyrene and epoxy resin) was raised with the dose because of pyrolysis of the polymer matrix in the vicinity of overheated particles [11-12]. A rise and further decline of the LII intensity of the rough carbon surface were observed with an increase in the number of irradiating laser pulses [15]. This feature of LII of rough surfaces was in good agreement with the calculation results and could be explained based on the models of (i) non-uniform heating of the surface asperities; (ii) dominant carbon evaporation from the tops of asperities; (iii) laser-induced undersurface pore expansion.

It should be noted that various porous structures of carbon materials caused strong differences in their thermal conductivity, which was changed in the range of 1 to 100 W/(m·K) [18] and influenced the LII signal. Moreover, the shape and duration of LII nanosecond pulses of carbon surfaces have not been sufficiently investigated. Thereby, in this work, the

Corresponding Author E-mail: czelenska@gmail.com

relaxation of LII nanosecond pulses of carbon superficial layers with different porosity and thermal conductivity has been studied.

2. Procedure

2.1. Carbon samples

The LII experiments were carried out using the samples of carbon electrode rods with porosity of approximately 25% (determined by measuring the material density). The obtained value of graphite electrode porosity was consistent with the reference data, which showed the porosity value for this type of an electrode in the range of 20-30% [18]. Two types of the samples of carbon superficial layers were prepared: a cleavage of a carbon electrode with the rough surface (low-porous carbon superficial layer) and polished surface covered by graphitic flakes (high-porous carbon superficial layer). The rough carbon surface was obtained by breaking the carbon rod along the cleavage plane. The polishing procedure included dry grinding of the carbon rod with an abrasive surface and dry polishing with a soft surface (paper, fabric) until the sample surface becomes specular (inspected visually). In this case, the smooth surface covered by graphitic flakes was formed.

High porosity and, as a result, low thermal conductivity, of a superficial layer of the polished carbon surface were due to a graphitic flake-like nanostructure containing nanocavities between flakes and the roughness value was estimated as tens of nm. At the same time, the thermal conductivity of a superficial layer of the untreated carbon surface (a cleavage of a carbon rod) was higher than that of the polished surface covered by flakes.

2.2. Experimental details

LII of the carbon samples was excited by a Q-switched YAG:Nd^{3+} laser (λ = 1064 nm, τ = 20 ns, intensity was 5-10 MW/cm^2). A simplified experimental setup of laser heating of the carbon samples and measurements of the LII pulses is shown in Fig. 1. A LII signal was collected by an optical fiber bundle and supplied to a photomultiplier through optical filters. Photosignals were measured in the linear photoresponse range of a photomultiplier 14ЭЛУ-ФС (spectral sensitivity region is 300-700 nm with the maximum sensitivity at 400 nm, time resolution is 1.3 ns). LII oscillograms were detected at a fixed wavelength λ_{LII} = 400 nm. The kinetics of LII of the carbon samples with a rough cleavage and polished surface was studied.

2.3. Calculation

The computer simulation of laser heating and LII of the carbon surfaces was based on the thermal conduction equation:

$$div\big(k\ gradT(\vec{r},t)\big) + W(\vec{r},t) = C_p \frac{dT(\vec{r},t)}{dt}, \qquad (1)$$

where $T(\vec{r},t)$ is the local temperature at a point with coordinates $\vec{r}$ inside the sample at a point of time t, k is the thermal conductivity coefficient of carbon, C_p is the heat capacitance of carbon, $W(\vec{r},t) = \alpha F(\vec{r},t)$ is the heat source function, where $\alpha = 10^5$ cm^{-1} is the absorption coefficient of carbon at the laser wavelength λ = 1064 nm [19], and $F(\vec{r},t)$ is the local laser intensity.

The laser pulse shape was taken as the following Gauss function:

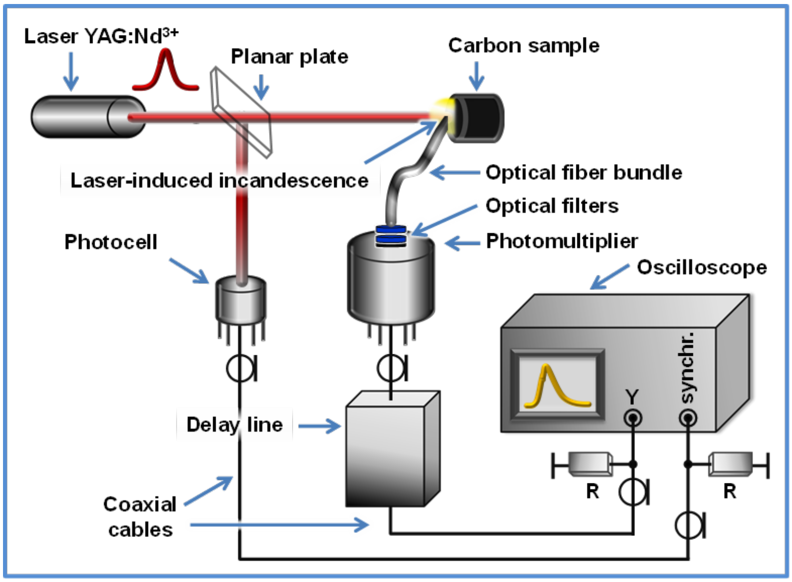

Fig. 1. Simplified experimental setup of LII measurements.

$$F = F_0 e^{-4ln2(\frac{t}{\tau_i})^2}, \tag{2}$$

where F_0 is the peak intensity of the incident laser beam, τ_i = 20 ns is the laser pulse duration.

The laser intensity decreases along the beam axis Z according to the following equation:

$$\frac{dF}{F} = -\alpha\, dz. \tag{3}$$

The LII intensity I_t was calculated by integration of Plank's blackbody emission function:

$$i_\lambda = \frac{const \cdot \lambda^{-5}}{e^{\frac{\xi}{\lambda T}} - 1}, \tag{4}$$

over the irradiated surface of a sample:

$$I_t = \iint_S i_\lambda dS, \tag{5}$$

where $const$ is incorporated in the coefficient group of constants, $\xi = {hc}/{k_B}$ =1.4388 nm·K, h is the Planck's constant, c is the speed of light, k_B is the Boltzmann constant, λ is the wavelength of LII detection, dS is the differential of the surface area S.

The LII signal was collected at a fixed wavelength of 400 nm and the maximal local temperature of the irradiated surface was adjusted to the value of 4000 K. This temperature was achieved by selecting the corresponding laser pulse intensity. Thermal conductivity k and absorption coefficient α of light-absorbing material were variable parameters in the calculations.

The optical and thermal parameters of carbon and air used in the calculations have been taken from the literature and shown in Table 1 [19-22].

The thermal conductivity value of carbon materials varies widely and depends on the heat propagation direction. Considering the effect of the porous structure of a sample on the heat transmission, for the simulation of laser heating of a carbon superficial layer formed with graphitic flakes (polished samples), one of the lowest values of thermal conductivity (6 W/(m·K)) was chosen, which was typical for high-porous carbon materials. For the solid samples (cleavage of a carbon rode), the highest value of thermal conductivity (100 W/(m·K)) was chosen which corresponded to the ideal carbon material and was more typical for carbon electrodes.

Table 1. Optical and thermal parameters of carbon and air used in the calculations

Material	Absorption coefficient, α [m^{-1}]	Thermal conductivity, k [W/(m·K)]	Heat capacity, C_p [J/(m^3·K)]
High-porous carbon (polished carbon surface)	$1\cdot10^7$	6	$1.6\cdot10^6$
Low-porous carbon (cleavage of a carbon rod)	$1\cdot10^7$	100	$1.6\cdot10^6$
Air	0	$3.7\cdot10^{-2}$	1320

3. Results and Discussion

The results of the oscilloscope measurements of the LII pulses emitted by the polished carbon surface (a) and cleavage of a carbon rod (b) are presented in Fig. 2

As seen from Fig. 2 and Table 2, the width at the half-height of the LII pulse of the polished carbon surface with the high-porous superficial layer is 21 ns, and the LII pulse duration (FWHM) for the cleavage of a carbon rod with the low-porous superficial layer is 14.6 ns. The shorter FWHM in the case of cleavage of a carbon rod (Fig. 2b) is associated with the material, which more efficiently removes heat from the laser-heated thin superficial layer according to the equations (1) and (3).

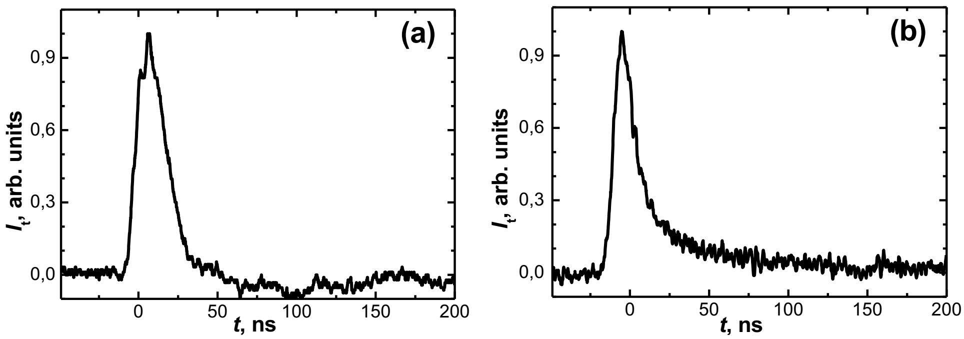

Fig. 2. Oscillograms of nanosecond LII pulses emitted by the polished carbon surface (a) and cleavage of a carbon rod (b).

Having approximately the same rise time of the LII signals for both kinds of the carbon superficial layers, the LII pulse relaxation time differs considerably. The decay time of the LII pulse of the low-porous carbon superficial layer is almost twice higher in comparison with the relaxation time of the LII pulse of the high-porous superficial layer that can be explained by the low thermal conductivity coefficient (about 1-10 W/(m·K)) for the high-porous material.

An impact of thermal conductivity of the superficial layer of the carbon sample on the LII pulse duration can be confirmed by the calculations based on the simplified model described in Section 2. However, the proposed model does not explain the observed tail of the LII pulse (Fig. 2a, b). The typical calculated oscillograms of the LII signals are presented in Fig. 3. The corresponding values of the coefficients of thermal conductivities, laser power densities and LII pulse durations are shown at the arrows (Fig. 3).

Table 2. Time parameters of the LII pulses of the different samples obtained from the oscillograms shown in Fig.2.

LII pulse time parameter	Time for oscillogram (a), [ns]	Time for oscillogram (b), [ns]
Pulse duration	21	14.6
Rise time (from $0.1I_t$ to $0.9I_t$)	10.4	9.2
Relaxation time (from $0.9I_t$ to $0.1I_t$)	21.6	45

An impact of thermal conductivity of the superficial layer of the carbon sample on the LII pulse duration can be confirmed by the calculations based on the simplified model described in Section 2. The typical calculated oscillograms of the LII signals are presented in Fig. 3. The corresponding values of the coefficients of thermal conductivities, laser power densities and LII pulse durations are shown at the arrows (Fig. 3).

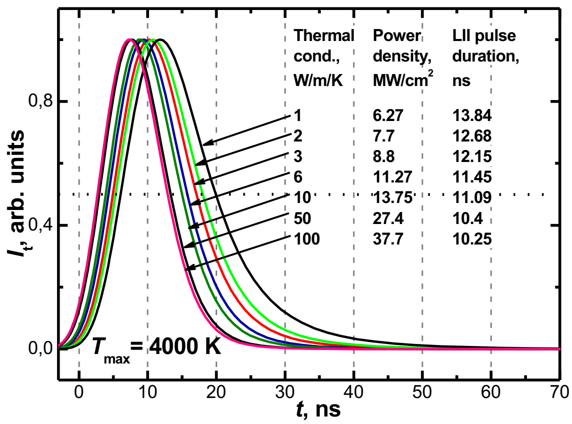

Fig. 3. Calculated oscillograms of the nanosecond LII pulses of the flat carbon surface with different thermal conductivity coefficients.

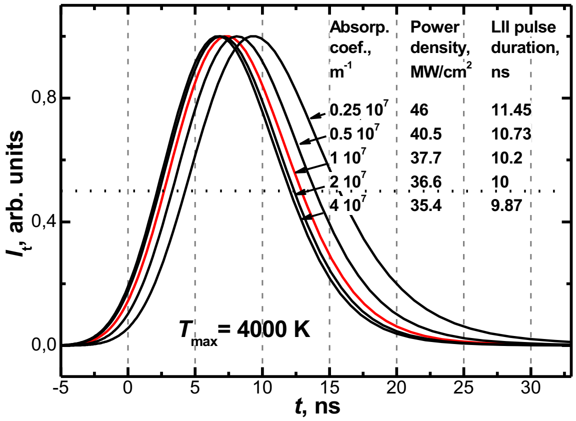

Fig. 4. Calculated oscillograms of the nanosecond LII pulses of the flat carbon surface with different absorption coefficients.

The ratio of the values of the LII pulse durations is preserved for both the experimental results and calculations. Duration of the LII pulse for the low-porous carbon sample is one-third less than that of the LII pulse emitted by the high-porous carbon superficial layer.

The LII pulse durations obtained from the experiments (Fig. 2 and Table 2) are higher than the values obtained by computer simulations. The disagreement can be due to the using of the values of heat capacity and absorption coefficient taken from the literature that can differ from the corresponding parameters of the studied samples. For example, an increase in the absorption coefficient leads to a decrease in the LII pulse duration as seen from Fig. 4.

In addition, the actual thermal parameters of materials depend on temperature, thus, the considering of these value as constants also contributes to the inaccuracy in the calculations. For finer calculations, more specific optical and thermal parameters of the investigated samples should be used with taking into account their temperature dependences. In particular, the appropriate data are unavailable in the necessary temperature range. Also, microscopic features of generation of LII signals, including high non-uniformity of distribution of temperature over the irradiated surface, have not been considered. In fact, the calculation model explains just the tendency of thermal conductivity impact on LII pulses: if thermal conductivity is higher, heat is removed faster hence, the LII pulse is shorter.

4. Conclusion

The difference in thermal conductivity of the carbon superficial layers with low and high porosity resulted the changes in shape and duration of the LII pulses excited by nanosecond laser radiation. Due to low thermal conductivity and slow heat transfer into the bulk of the material, the porous carbon superficial layer had a longer relaxation of the LII signal that was exhibited in a prolonged decay of the LII pulse. Thus, the experimental results and calculations have shown that the porosity of the material significantly affected the relaxation time of the LII emission, hence LII can be considered as an indicator of presence of undersurface cavities, pores, voids or inclusions with different thermal conductivity coefficients.

Acknowledgements

This research was partly supported by 2016 and 2017 Cooperative Research Projects at Research Institute of Electronics, Shizuoka University (Grants No 2054, 2055, 2013 and 2014).

References

[1] L.A. Melton, Soot diagnostics based on laser heating, *Applied Optics* 23 (1984) 2201-2208.
[2] R.L. Vander Wal, Laser-induced incandescence: detection issues, *Applied Optics* 35 (33) (1996) 6548-6559.
[3] B. Mewes and J.M. Seitzman, Soot volume fraction and particle size measurements with laser-induced incandescence, *Applied Optics* 36 (1997) 709-717.
[4] R.L. Vander Wal, T.M. Ticich and A.B. Stephens, Can soot primary particle size be determined using laser-induced incandescence? *Combustion and flame* 116(1) (1999) 291-296.
[5] S. Will, S. Schraml and A. Leipertz, Comprehensive Two-Dimensional Soot Diagnostics Based on Laser-Induced Incandescence (LII), *Symposium (International) on Combustion* 26 (1996) 2277-2284.
[6] H.A. Michelsen, C. Schulz, G.J. Smallwood and S. Will, Laser-induced incandescence: Particulate diagnostics for combustion, atmospheric, and industrial applications, *Progress in Energy and Combustion Science* 51 (2015) 2-48.
[7] K. Mansour, M.J. Soileau and E.W. Van Stryland, Nonlinear optical properties of carbon-black suspensions (ink), *Journal of the Optical Society of America B* 9(7) (1992) 1100-1109.
[8] R. Sommer and A. Leipertz, Application of laser-induced incandescence to suspended carbon black particles, *Optics Letters* 32(13) (2007) 1947-1949.
[9] S. Zelensky, Laser-induced heat radiation of suspended particles: a method for temperature estimation, *Journal of Optics A: Pure and Applied Optics* 1 (1999) 454-458.
[10] Ju.Ju. Rulik, N.M. Mikhailenko, S.E. Zelensky and A.S. Kolesnik, Laser-induced incandescence in aqueous carbon black suspensions: the role of particle vaporization, *Semiconductor Physics, Quantum Electronics & Optoelectronics* 10(2) (2007) 6-10.
[11] S. Zelensky, A. Kolesnik, A. Kopyshinsky, V. Garashchenko, K. Zelenska, V. Stadnytsky and E. Shinkarenko, Thermal emission of carbon microparticles in polymer matrixes under pulsed laser excitation, *Ukrainian Journal of Physics* 54(10) (2009) 983-988.
[12] K. Zelenska, S. Zelensky, L. Poperenko, K. Kanev, V. Mizeikis and V. Gnatyuk, Thermal mechanisms of laser marking in transparent polymers with light-absorbing microparticles, *Optics & Laser Technology* 76 (2016) 96-100.
[13] S. Zelensky, Laser-induced heat radiation in borate glass, *Journal of Physics: Condensed Matter* 10 (1998) 7267-7272.
[14] A.V. Kopyshinsky, Y.P. Lazorenko and S.E. Zelensky, Laser induced incandescence of borate glass doped with carbon microparticles, *Functional materials* 18(1) (2011) 116-120.
[15] S. Zelensky, L. Poperenko, A. Kopyshinsky and K. Zelenska, Nonlinear characteristics of laser-induced incandescence of rough carbon surfaces, *Nonlinear Optics and Applications VI*, *Proceedings of SPIE* 8434 (2012) 84341H-1-6.

[16] K. Zelenska, S. Zelensky, A. Kopyshinsky, S. Rozouvan and T. Aoki, Laser-induced incandescence of rough carbon surfaces, *JJAP Conference Proceedings* 4 (2015) 011106-1-6.
[17] A.V. Kopyshinsky, S.E. Zelensky, E.A. Gomon, S.G. Rozouvan and A.S. Kolesnik, Laser-induced incandescence of silicon surface under 1064-nm excitation, *Semiconductor Physics, Quantum Electronics & Optoelectronics* 15(4) (2012) 376-381.
[18] M.I. Rogaylin and E.F. Chalyh, Handbook of carbon materials, Chemistry, Leningrad, 1974.
[19] H-J. Hagemann, W. Gudat and C. Kunz, Optical constants from the far infrared to the x-ray region: Mg, Al, Cu, Ag, Au, Bi, C, and Al_2O_3, *Journal of the Optical Society of America* 65(6) (1975) 742-744.
[20] H.O. Pierson, Handbook of carbon, graphite, diamond and fullerenes: processing, properties and applications, Noyes Publications, Park Ridge, New Jersey, 1993.
[21] J. Lee, J. Kim and T. Hyeon, Recent progress in the synthesis of porous carbon materials, *Advanced Materials* 18(16) (2006) 2073-2094.
[22] D.W. Wang, F. Li, M. Liu, G.Q. Lu and H.M. Cheng, 3D aperiodic hierarchical porous graphitic carbon material for high-rate electrochemical capacitive energy storage, *Angewandte Chemie International Edition* 47(2) (2008) 373-376.